Characterization of Graphene Oxide by Flow Cytometry and Assessment of Its Cellular Toxicity

Article *in* Journal of Biomedical Nanotechnology · February 2011

DOI: 10.1166/jbn.2011.1186 · Source: PubMed

CITATIONS
16

READS
136

6 authors, including:

Sunil Kumar Singh
Central University of Punjab
38 PUBLICATIONS **1,020** CITATIONS
SEE PROFILE

Manoj Kumar Singh
University of Aveiro
105 PUBLICATIONS **3,433** CITATIONS
SEE PROFILE

Dr. Manasa K. Nayak
University of Iowa, Iowa City, USA
26 PUBLICATIONS **394** CITATIONS
SEE PROFILE

Sharda Kumari
University of Texas Southwestern Medical Center
16 PUBLICATIONS **290** CITATIONS
SEE PROFILE

CARBON 49 (2011) 684–692

available at www.sciencedirect.com

ScienceDirect

journal homepage: www.elsevier.com/locate/carbon

Size distribution analysis and physical/fluorescence characterization of graphene oxide sheets by flow cytometry

Sunil K. Singh [a], *Manoj K. Singh* [b], *Manasa K. Nayak* [a], *Sharda Kumari* [a], *José J.A. Grácio* [b], *Debabrata Dash* [a,*]

[a] *Department of Biochemistry, Institute of Medical Sciences, Banaras Hindu University, Varanasi 221005, India*
[b] *Center for Mechanical Technology and Automation, University of Aveiro, Aveiro 3810-193, Portugal*

ARTICLE INFO

Article history:
Received 7 August 2010
Accepted 13 October 2010
Available online 20 October 2010

ABSTRACT

Flow cytometry is presented here as an alternative tool for analysis of size distribution and intrinsic fluorescence of graphene oxide (GO) sheets. Unlike other nanoparticles, GO sheets induced scatter signals reasonably distinct from the background noise of the system. The number of gated signals generated by the sheets was proportional to GO concentration, indicating that non-spherical particles like GO can be convincingly studied by flow cytometry. The asymmetry in forward scatter-side scatter contour plots was consistent with a non-uniform size distribution of individual sheets in the population, which contrasted with a prototype animal cell population. GO was endowed with intrinsic fluorescence detectable through the three fluorescence channels in the cytometer and allowed comparison of relative fluorescence intensities associated with individual sheets. Flow cytometry thus provides rapid access to high-dimension statistical information on individual GO sheets that is not achievable with existing characterization tools, and may prove to be an indispensable tool in graphene research.

1. Introduction

Graphene is a two-dimensional new allotrope of carbon, distinctly different from carbon nanotubes and fullerenes that has become one of the most exciting topics of research within the last 5 years. Graphene ideally consists of a single layer of carbon atoms and is of micron dimension with thickness in range of nanometers [1,2]. Pristine single-layer graphene sheets were initially produced by the scotch-tape method in 2004 [3], which also generated samples composed of two or more atomic layers. However, the process has inherent disadvantages in terms of yield and throughput. An effective approach in this regard was based on chemical exfoliation of graphite to GO [4]. The resultant material consists of graphene-derived sheets and is heavily oxygenated with hydroxyl, carbonyl and carboxylic functional groups [5,6]. Thus, the hydrophilic GO sheets can remain as highly stable aqueous dispersions with enormous application potential in biomedical field [7–11]. Their remarkable features like large surface area, high conductivity, electron mobility, stability and optical properties are associated with thickness and number of layers involved in GO sheets [12–14]. Characterization of physical properties of individual GO sheets in a population is a significant quality control assay determining suitability of the preparation in various applications [15].

Dimension and thickness of GO layers are usually analyzed by atomic force microscopy, as well as optical or electron microscopy [6]. However, information on statistical evaluation of wide size distributions or inherent intrinsic fluorescence of individual GO sheets is not readily available from such images. Although dynamic light scattering has been employed for characterization of submicron particles,

* *Corresponding author:* Fax: +91 542 2367568.
E-mail address: ddass@satyam.net.in (D. Dash).
0008-6223/$ - see front matter
doi:10.1016/j.carbon.2010.10.020

the tool has limitation that it is more suitable for spherical and homogeneous particles [16]. Further, size and physical properties of individual graphene sheets (in a GO population) cannot be evaluated with this approach. To circumvent these problems, reliable and robust techniques are needed that can reproducibly characterize graphene within a short period.

Flow cytometry is a technique that integrates light scattering and fluorescence signals emanated from a group of cells or particles in the path of laser beam, thereby generating extensive statistical data on size, shape and internal characteristics of individual cells within the population. The method has found wide applications in biological research in view of its predilection for multi-parameter analysis at the single-cell level. Flow cytometry usually characterizes cells or particles with typical size range between 0.5 and 70 μm. Scatter signals evoked by submicron nano-sized particles are obligatorily gated along with the background noise, thereby blurring the distinction between noise and signal, which precludes flow cytometric analysis of nanoparticles unless particles are aggregated to larger dimension or have been made fluorescent. Here we, for the first time, report that scatter signals generated by native single or few-layer GO sheets in a flow cytometer are gated distinctly apart from the background sheath fluid noise, thus enabling extensive analysis of size distribution and characterization of fluorescence properties of individual GO sheets in the population. The results show that GO sheets are asymmetric in size and are endowed with intrinsic fluorescence detectable through the three fluorescence channels (FL1, FL2 and FL3) in the flow cytometer. Flow cytometer may, therefore, prove to be an indispensable tool in graphene research, which can have applications in exploring biomedical potential of this new material in miscellaneous areas like imaging, graphene–cell interaction as well as drug delivery.

2. Experimental details

2.1. Materials

Human thrombin, apyrase, ethylenediaminetetraacetic acid (EDTA), acetylsalicylic acid, graphite powder and other reagents were procured from Sigma. All other reagents were of analytical grade.

2.2. Graphene preparation

GO was prepared by refluxing commercially obtained graphite powder with a strongly acidic mixture of sulfuric and nitric acid, by using modified Hummers method which is described elsewhere [17]. The resultant suspension was intensively washed with distilled water by filtration and then by centrifugation in order to remove residual unexfoliated graphite and further oxidant agents. Fourier transform infrared spectroscopy (FT-IR) analysis (Supplementary information Fig. S1a) confirmed the presence of carboxylic groups (~1729 cm^{-1}) at the GO surface, which is responsible for the colloidal nature of graphene in aqueous solution.

2.3. Characterization of GO

The surface morphology of exfoliated graphene samples was examined by field-emission scanning electron microscopy (FE-SEM) (Hitachi S-800, and SU-70, 30 keV) and optical microscopy (Nikon model Eclipse LV150). The sample topography and thickness measurement of exfoliated GO were performed by NanoScope IIIA (Digital Instruments) atomic force microscope (AFM) in tapping mode. FT-IR spectra were recorded from KBr pellets (Aldrich, 99%, FT-IR grade) using a Mattson 7000 FT-IR spectrometer with resolution 8 and 256 interferograms. The crystallinity and quality of as-synthesized GO sheets were analyzed by a conventional high-resolution transmission electron microscope (HR-TEM) (JEOL 2200F TEM/STEM). Fluorescence measurements of GO sheets were performed on Hitachi fluorescence spectrophotometer (model F-2500) using FL Solutions software. GO sheets were excited at 400 nm and emission spectra were recorded in the range of 500–750 nm using 10/5 nm slit widths.

2.4. Platelet preparation

Platelets were isolated from fresh human blood by differential centrifugation, as already described [18]. Briefly, Blood from healthy volunteers was collected in citrate–phosphate–dextrose adenine and centrifuged at 180*g* for 10 min. PRP (platelet-rich plasma) was incubated with 1 mM acetylsalicylic acid for 15 min at 37 °C. After addition of EDTA (5 mM), platelets were sedimented by centrifugation at 800*g* for 15 min. Cells were washed in buffer A (20 mM HEPES, 138 mM NaCl, 2.9 mM KCl, 1 mM $MgCl_2$, 0.36 mM NaH_2PO_4, 1 mM EGTA (ethylene glycol tetraacetic acid), supplemented with 5 mM glucose and 0.6 ADPase units of apyrase/ml, pH 6.2). Platelets were finally resuspended in buffer B (pH 7.4), which was the same as buffer A but without EGTA and apyrase. The final cell count was adjusted to $0.5–0.8 \times 10^9$/ml. Morphology of the cells was studied under fluorescence microscope with phase contrast attachment (Nikon model Eclipse Ti-E, Towa Optics, India) and viability of platelets was examined with Whole Blood/Optical Lumi-Aggregometer (Chrono-log model 700-2, Wheecon Instruments, India). All steps were carried out under sterile conditions and precautions were taken to maintain the cells in resting state.

Table 1 – Flow cytometer settings used for size distribution analysis of GO in solution. All gains were logarithmic. FSC and SSC, optical scattering channels; FL1, green fluorescence channel; FL2, orange fluorescence channel; FL3, dark red fluorescence channel; FL4, red fluorescence channel (expressed as volts).

Sample	Threshold (FSC-H)	Detector setting					
		FSC-H	SSC-H	FL1-H	FL2-H	FL3-H	FL4-H
GO	52	E00	350	600	550	650	680

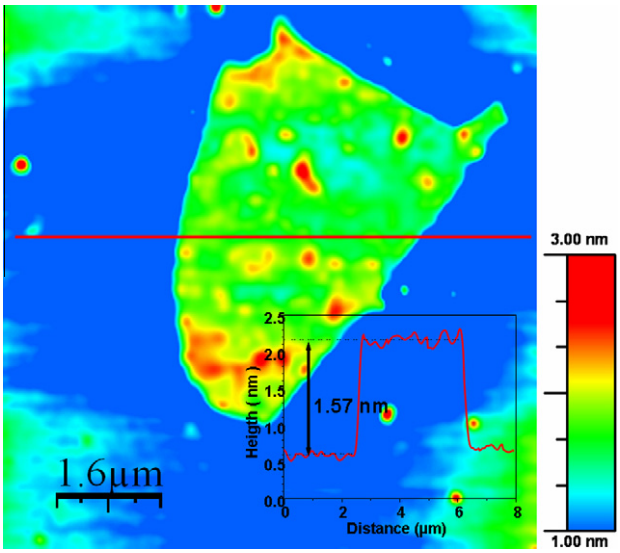

Fig. 1 – AFM images of GO sheet in tapping mode. The insets show the corresponding height profile.

2.5. *Flow cytometry*

Suspensions of GO as well as platelets were diluted with sheath fluid and analyzed with FACSCalibur flow cytometer (Becton Dickinson India Pvt. Ltd., Gurgaon) fitted with two excitation sources, 488 nm (air cooled argon-ion laser) and 632 nm (red diode laser), using Cell Quest Pro software. Forward scatter (FSC) and side scatter (SSC) optical signals, which respectively represent size and granularity of the particles, were acquired in logarithmic scale using primary data acquisition mode. Changes in these particle parameters will modify the quantum of laser light diffracted or scattered, thus causing altered population distribution in FSC–SSC planes. Intensity of fluorescence emission was detected on four separate detectors, labeled FL1, FL2, FL3 and FL4, each with its own set of wavelength filters and data were presented in form of histograms. Gate was imposed on the GO population for exclusive analysis. Events were acquired by using collection criteria of the software either to stop acquisition after 10,000 events acquired (event limit) or after 10 s has elapsed (time limit). Flow cytometric settings used for size distribution analysis of graphene are presented in Table 1.

To determine if two overlaid histograms represent different populations, Kolmogorov–Smirnov (K–S) statistics [19] (Cell Quest Pro acquisition-analysis software) was applied to histograms representing either FSC or SSC population. The computation uses $D/s(n)$ ratio, where $s(n)$ equals the square root of $(n_1 + n_2)/(n_1 \times n_2)$, n_1 is the number of events in the first histogram and n_2 is the number of events in second histogram. D denotes the K–S statistic (greatest difference between the two curves). All fluorescence data were collected using four-decade logarithmic amplification. Total number of events analyzed for each sample was 10,000. The results were representative of 4–5 independent experiments.

3. Results and discussion

The as-synthesized GO sheets were initially examined by optical microscopy and FE-SEM (Supplementary information: Fig. S1b–d). In addition, we performed AFM measurements to analyze overall sample topography, and also to identify the number of layers of GO sheets. From the surface characterization studies we concluded that, the exfoliated GO sheets in our preparation were in the order of 0.5–5 μm, and thickness is ~1.5 nm (between 2 and 3 layers) (Fig. 1). However, this technique has a very slow throughput. In addition, an instrumental offset of ~0.5 nm (caused by different interaction forces) always exists, which is even larger than the thickness

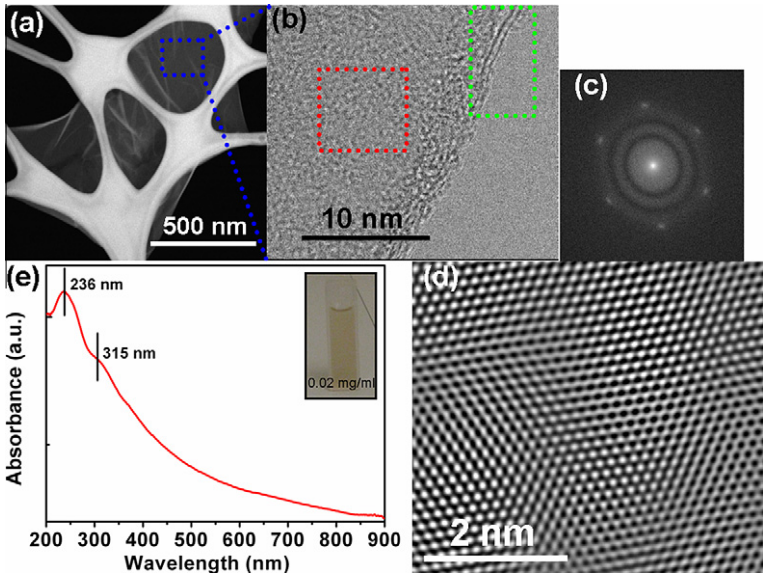

Fig. 2 – (a) Bright-field TEM image of suspended GO sheet on copper grid. (b) HR-TEM image of the blue dotted area denoted in a. (c) 2D FFT performed in the region indicated with red box exhibiting perfect crystallinity of GO sheet. (d) HR-TEM image reveals honeycomb structure of graphene sheet performed at the area denoted by red dotted line. (e) UV–vis absorbance spectra of GO solution in water. Inset shows the color of the GO solution (0.02 mg/ml).

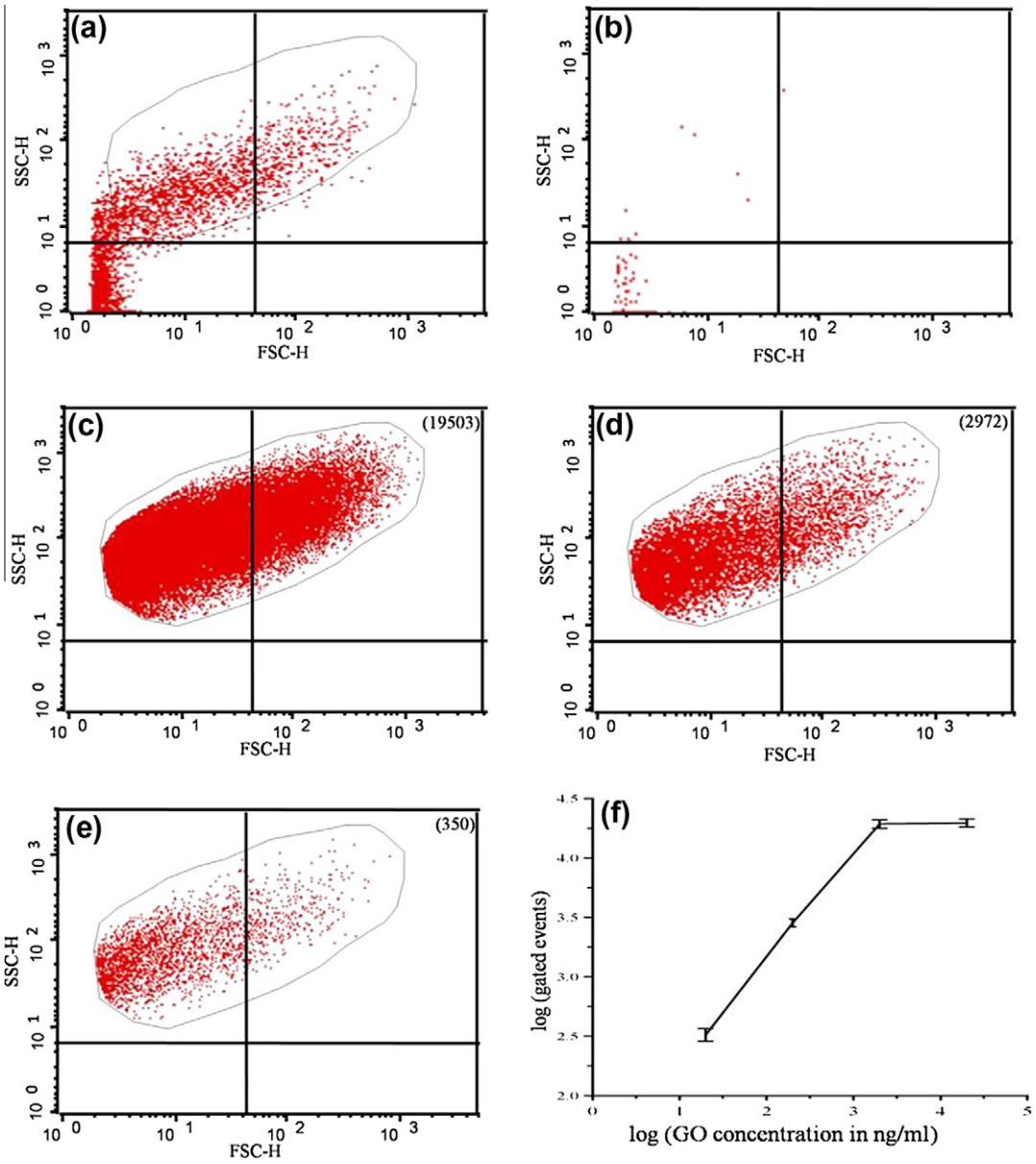

Fig. 3 – FSC–SSC dot plot displaying size and properties of GO population. (a) and (b) Represent GO (20 μg/ml) and sheath fluid, respectively. Events from graphene at different dilutions (2, 0.2 and 0.02 μg/ml) were acquired for 10 s at constant flow rate (c–e, respectively). Number of gated events at each dilution of GO is stated within brackets (c–e). (f) Represents logarithmic plot between gated events (mean ± SD) and concentrations of GO. The results were representative of four independent experiments.

of a graphene monolayer. Thus, data fitting is required to extract the true thickness of the GO sheets [20].

HR-TEM studies were performed to examine crystallinity and quality of as-synthesized GO sheets. For this, samples were prepared by dipping a carbon-coated copper grid into the (GO/water) solution and allowing it to dry. Fig. 2a shows a bright-field TEM image of GO sheet attached to a copper grid. The suspended graphene membranes consist of single-layer or bilayer sheets with average 2 μm dimension. The HR-TEM image performed from the blue dotted region (Fig. 2a) clearly showed two-layered graphene (two graphene layers separated by 0.40 ± 0.02 nm) and it is marked by green dotted area in Fig. 2b. A 2D fast Fourier transform (FFT) (Fig. 2c) was performed in the region indicated by a red box in Fig. 2b, which shows crystalline nature of bilayer graphene sheet. The corresponding HR-TEM image also reveals honeycomb structure of graphene sheet (Fig. 2d).

The as-synthesized GO consisting of several mono-layers (yellowish brown color, see inset of Fig. 2e) exhibited optical absorption in the visible and near-infrared range. The maximum absorbance at 230 nm could originate from π–π^* transition of aromatic sp^2 domains [3,21] whereas a minor peak at ~320 nm was attributable to n–π^* transitions of C=O (Fig. 2e) [22]. The inherent optical properties and stable nature of GO suspensions could facilitate biomedical research in areas of cellular imaging and drug delivery.

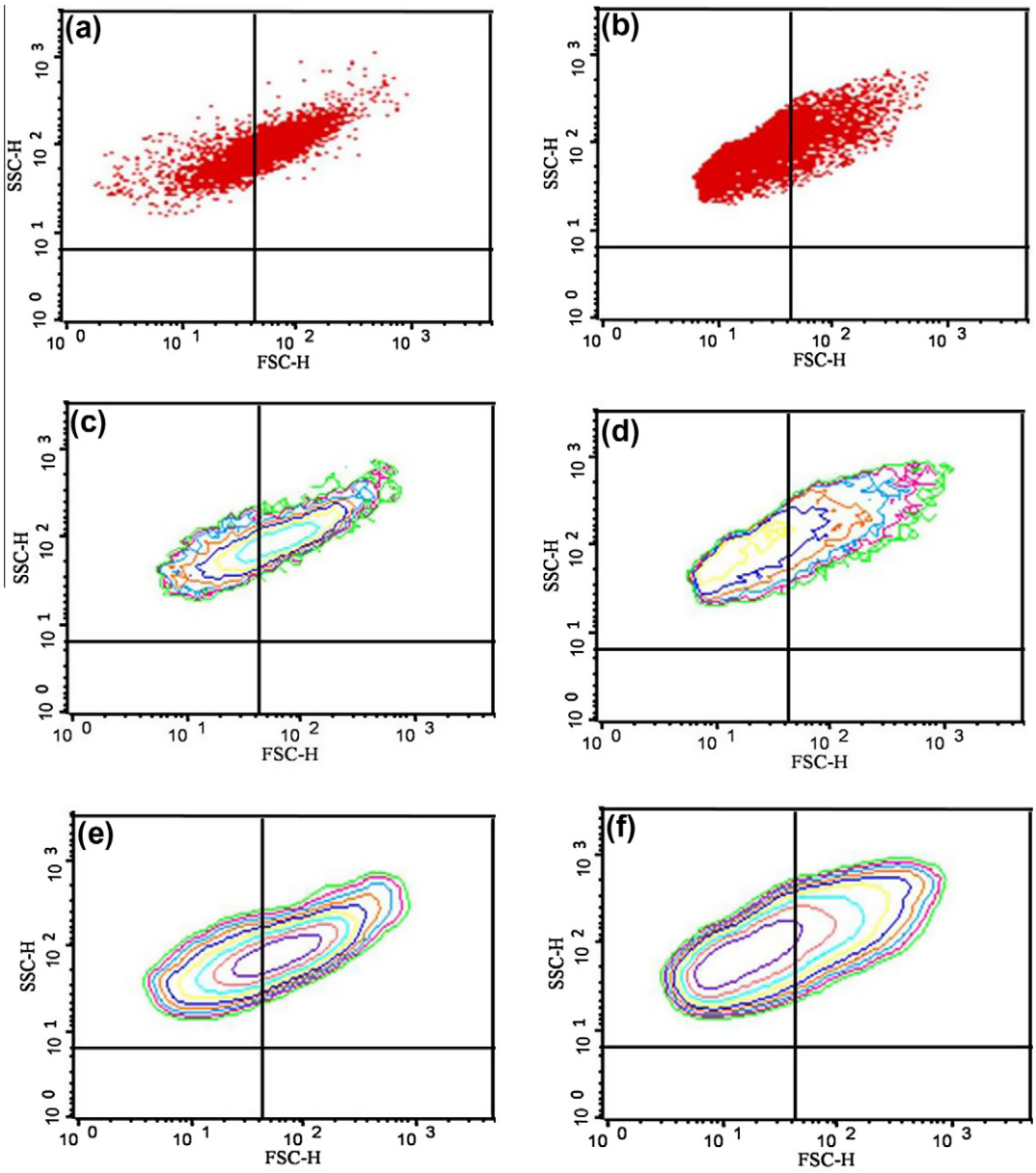

Fig. 4 – (a) and (b) Represent dot plots of platelets and GO, respectively, under identical gating. (c) and (d) Represent corresponding contour plots of platelets and GO, respectively. (e) and (f) Represent contour plots of platelets and GO, respectively, obtained after smoothening. The number of events analyzed was 10,000. The results were representative of five independent experiments.

For flow cytometric analysis, FSC and SSC parameters of GO population were acquired and displayed in the dot plot acquisition quadrants (Fig. 3). Sheath fluid was mobilized to determine background signal or noise. By adjusting FSC and SSC detector voltages to E00 and 350 V, respectively, majority of GO population was found to be distributed in the upper quadrants (Fig. 3a) reasonably well distanced from background noise, while the latter was confined to the left lower quadrant close to the origin (Fig. 3b). However, some GO signals existed in the lower quadrant along with noise. Gate was imposed on the GO population present in both the upper quadrants for exclusive analysis. GO was serially diluted from 2 to 0.02 μg/ml and events were acquired for 10 s at each dilution. Number of gated events (dots) was found to decline progressively with decrease in GO concentration (Fig. 3c–f), indicating that GO sheets contributed to the signals. However, at high concentration of GO (>2 μg/ml), no further increment in events was observed (Fig. 3f). Thus, the results suggested that non-spherical particle like GO can be convincingly studied by flow cytometry within optimum concentration limits. Although a few earlier studies have attempted to evaluate submicron particles like liposomes [16,23] and silica nanoparticles [24] by flow cytometry, scatter signals emanating from them were not distinct from the background noise, thus rendering their analysis unconvincing and difficult.

We next evaluated changes in particle characteristics when GO existed at two different concentrations (2 and 20 μg/ml). Ten thousand events were acquired for each

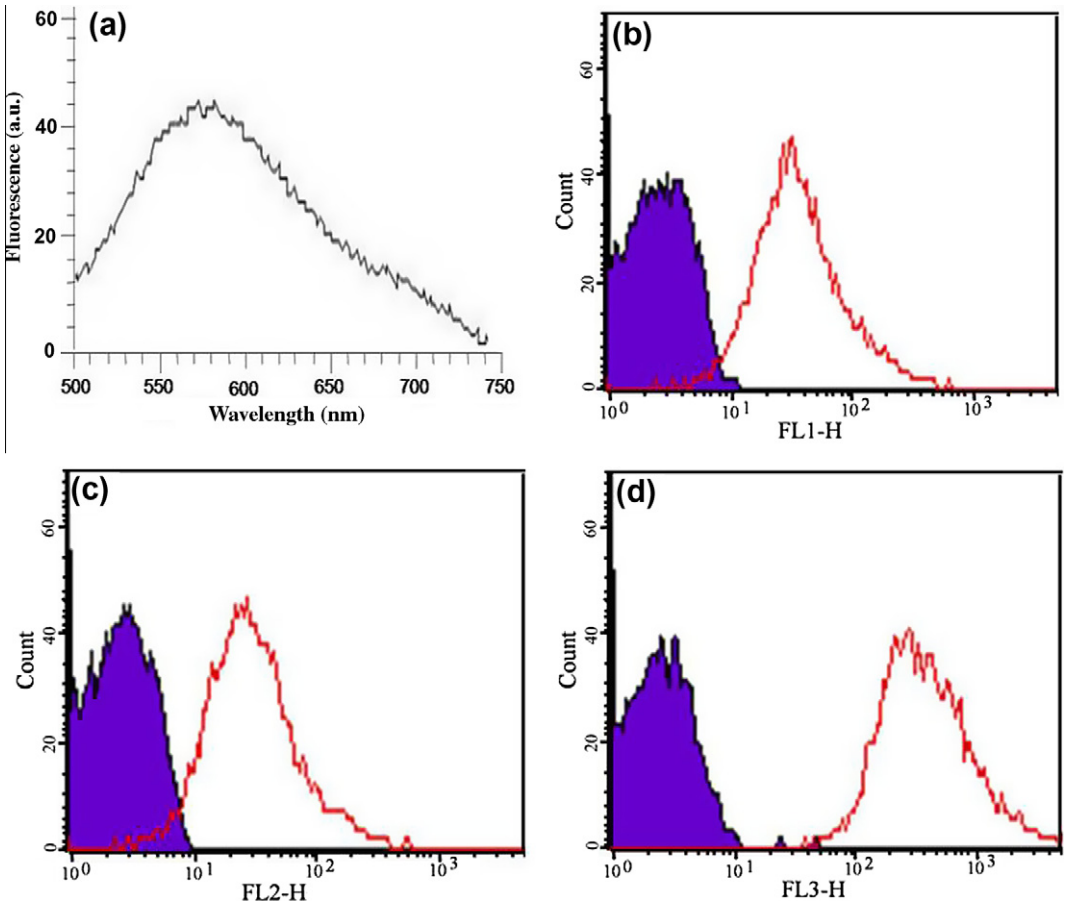

Fig. 5 – (a) Fluorescence spectrum of GO in the visible range. Excitation, 400 nm. (b–d) Overlaid histograms of platelets (shaded) and GO (unshaded). Histogram showed the level of fluorescence of platelet and GO populations in three different fluorescence channels as indicated. The number of events analyzed in each case was 10,000. The results were representative of five independent experiments.

dilution of graphene at constant flow rate and data were presented as FSC and SSC histograms (not shown). Histograms at both the concentrations of GO appeared identical and exactly superimposed, thus ruling out any difference in either FSC or SSC parameters at stated dilutions. Data were subsequently analyzed by employing K–S statistics [19]. The calculation computes summation of the histograms at either dilution and derives the greatest difference between them using $D/s(n)$ ratio (please refer to Section 2), which is the index of similarity between two curves. Thus, for example, when $D/s(n) = 0$, the populations are identical. From K–S analysis of SSC histograms of graphene at both concentrations, the D and $D/s(n)$ values were found to be 0.12 and 8.76 ($P < 0.001$), respectively, indicating significant change in the complexity of graphene particle upon dilution. This could be indicative of increased dispersion of graphene clusters in the medium upon dilution. Correspondingly, the D and $D/s(n)$ values for the FSC histogram were 0.09 and 6.30 ($P < 0.001$), respectively, indicating the drop in size of graphene clusters upon dispersion. Thus flow cytometry employing K–S analysis offers novel insight into complexity of particulate graphene under different experimental conditions, which is not hitherto discernible using other existing methods.

In order to establish a comparison between characteristics of GO and a cell type with identical gating parameter, flow cytometry was performed on freshly isolated and non-stimulated human blood platelets. Platelets are smallest blood cells having 1–3 μm diameter, which distribute and gate exactly similar to graphene in FSC–SSC dot plot (Fig. 4 a and b). Interestingly, distinct differences between platelets and graphene were observed when the events were presented as contour plots (Fig. 4c–f). Shape of contours was dramatically different in case graphene, which had an asymmetric distribution unlike the cells (Fig. 4 c and d). This observation was suggestive of existence of asymmetric population of graphene in the preparation contrasting homogeneity in blood platelets. Smoothening feature of the software was next exercised to decrease irregularities in the contour plot profile (Fig. 4 e and f) and contour lines were calculated on the basis of 50% logarithmic density. In Fig. 4e and f, the innermost contours represented 50% of peak height or population, while the next outer contour represented 25% peak height and so on. The corresponding percentages based on peak height were 50%, 25%, 12%, 6%, 3% and 1%. The innermost contour that represented majority of population was found to be located in upper right quadrant in case of cells (Fig. 4e) while it was shifted to upper left quadrant for graphene population (Fig. 4f). As left-shift in FSC–SSC plot corresponds to drop in particle size, this observation was consistent with the fact that, nearly 75% GO population was of smaller size compared

to the mean dimension of platelets (1–3 μm). This might be attributed to the fact that, majority of GO population was composed of single or few atomic layers, as evident from surface characterization analyses. Generally, the spacing of the contour lines indicates the nature of the population. Fig. 4e showed contour lines were evenly spaced or equidistant and close together indicating a uniform distribution of platelet population. Further, the asymmetric distribution or widely spaced contour lines in the upper right quadrant of Fig. 4f was suggestive of an abrupt jump in size of GO in about 15% of population. Thus, application of FSC–SSC contour plots yielded significant novel information on population distribution of GO, which was not evident with FSC–SSC dot plots or with other available techniques.

GO sheets are endowed with intrinsic fluorescence, which has found biological applications in areas like imaging and sensor development [15,25–27]. Consistent with these reports our GO preparation exhibited an emission peak at 575 nm upon excitation at 400 nm (Fig. 5a). We subsequently investigated intrinsic fluorescence of individual GO sheets using flow cytometry. Intensity of fluorescence emission was detected on three separate detectors, FL1, FL2 and FL3, each with its own set of wavelength filters (Fig. 5b–d). Non-fluorescent platelets were analyzed as the control. Majority population of GO was observed to have higher fluorescence intensity in all the three fluorescence channels. However, fluorescence was relatively stronger in FL3 region as compared to FL2 and FL1 channels. There was clear separation between histograms of GO and platelets in FL3, while the curves were closer with minor overlapping in other two channels. Overlapping of histograms indicated that, a minor population of GO remained non-fluorescent in FL2 and FL3. Next, we excited GO with 633 nm red laser and acquired emission in the range of FL4 filter. We found that histogram of GO overlapped upon that of the cells (Supplementary information: Fig. S2), indicating that GO was equally non-fluorescent as the cells in the FL4 range. Thus, FL3 appeared to be the most ideal for study of intrinsic fluorescence properties of graphene, whereas an external probe in the range of FL4 can be employed for analysis of dual fluorescence (for example, interaction of GO with a population of cells can be effectively studied when the latter is tagged with FL4-compatible fluorescent probe). As flow cytometry provides information on population distribution of GO endowed with different fluorescence intensities, the method is more relevant

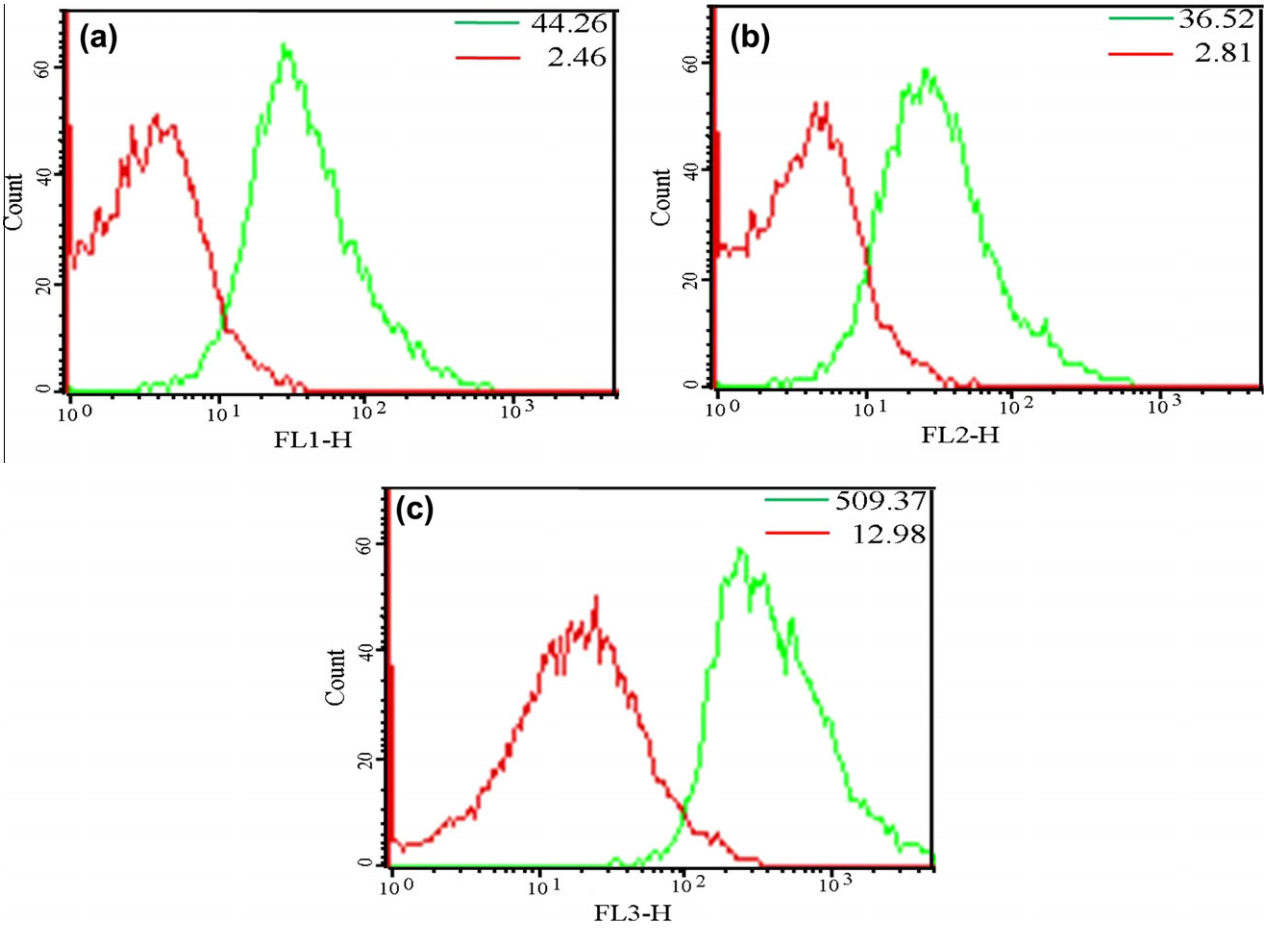

Fig. 6 – Histogram plots of GO sheets (green) and hydrazine vapor-treated GO (red). Overlaid histogram showed the level of fluorescence of the GO and hydrazine vapor-treated GO population in three different fluorescence channels as indicated. Median values for GO and hydrazine vapor-treated GO are stated within corresponding boxes. The results were representative of five independent experiments. (For interpretation of the references in colour in this figure legend, the reader is referred to the web version of this article.)

that simple fluorescence spectrophotometry, which generates the cumulative data of the sample without population statistics.

To further characterize intrinsic fluorescence of GO we exposed the material to hydrazine vapor for 5 min. Hydrazine-treated graphene was left-shifted in overlaid histograms as compared to untreated GO nanosheets (Fig. 6), indicative of significant quenching of fluorescence in presence of hydrazine. In histogram statistics median provides a good indication of the central tendency of the gated population. Significant difference in median values between GO and hydrazine-treated GO was observed in each fluorescence channel (Fig. 6), supportive of fluorescence quenching. Quenching may be attributed to removal of oxygen upon exposure to hydrazine leading to percolation among the sp^2 configurations of GO [28].

Techniques like TEM and AFM are well known for direct atomic resolution imaging of GO sheets; however, these methods are relatively more expensive and time consuming. Data on size distribution emanating from these methods will rely on observation of fewer GO sheets, which contrasts with the possibility of analyzing 50,000 or more events (sheets) by using flow cytometry. Methods like TEM and AFM are subjective and could easily be influenced by an observer bias. Flow cytometry has the unique advantage of simultaneous measurement of size distribution and fluorescence properties of GO sheets, which is not possible with the existing methods. Advanced flow cytometers equipped with cell sorting facility can separate as well as retrieve different homogeneous GO populations based on their size or fluorescence properties or other physical parameters. Thus, flow cytometry is more versatile than TEM, AFM and other available techniques in terms of rapidity, high sensitivity, ability to simultaneously evaluate size distribution and fluorescence properties, sorting different populations of GO and monitoring GO interaction with cells.

4. Conclusions

Flow cytometry can find a strong niche in nano research involving GO if not for other commonly studied nanoscale particles. Because of its unique ability to acquire scatter as well as multi-channel fluorescence emission signals emanated from individual GO sheets, this approach would add new dimension to conventional graphene characterization methods. Moreover, a flow cytometer with sorting capability can be employed to sort and retrieve different subpopulations of a GO preparation based on parameters like size, physical characteristics or fluorescence yield, thus opening up immense application possibilities with this versatile tool.

Acknowledgements

Grants received by D. Dash from the Department of Biotechnology (DBT), Government of India, and Indian Council of Medical Research (ICMR), and the equipment support from the DST Unit on Nanoscience and Technology (DST-UNANST), Banaras Hindu University, are gratefully acknowledged. We are thankful to T.A. Nagarjuna and Diwakar Sharma (Becton Dickinson India Pvt. Ltd., Gurgaon.) for their help and valuable suggestions on analysis of flow cytometric data. S.K. Singh and S. Kumari are recipients of research fellowships from the University Grants Commission (UGC), and Council of Scientific and Industrial Research (CSIR), India, respectively. M.K. Singh would like to thank the Ciencia 2007 Program, Foundation of Science and Technology (FCT – Portugal) and facility RNME – Pole University of Aveiro. The authors dedicate this work to Prof. C.N.R. Rao, Jawaharlal Nehru Centre for Advanced Scientific Research, who has pioneered graphene research in India.

Appendix A. Supplementary data

Supplementary data associated with this article can be found, in the online version, at doi:10.1016/j.carbon.2010.10.020.

REFERENCES

[1] Tung VC, Allen MJ, Yang Y, Kaner RB. High-throughput solution processing of large-scale graphene. Nat Nanotechnol 2009;4:25–9.
[2] Singh MK, Titus E, Goncalves G, Marques PAAP, Bdikin I, Kholkin AL, et al. Atomic-scale observation of rotational misorientation in suspended few-layer graphene sheets. Nanoscale 2010;2:700–8.
[3] Novoselov KS, Geim AK, Morozov SV, Jiang D, Zhang Y, Dubonos SV, et al. Electric field effect in atomically thin carbon films. Science 2004;306:666–9.
[4] Park S, Ruoff RS. Chemical methods for the production of graphenes. Nat Nanotechnol 2009;4:217–24.
[5] Goncalves G, Marques PAAP, Granadeiro CM, Nogueira HIS, Singh MK, Gracio J. Surface modification of graphene nanosheets with gold nanoparticles: the role of oxygen moieties at graphene surface on gold nucleation and growth. Chem Mater 2009;21:4796–802.
[6] Mkhoyan KA, Contryman AW, Silcox J, Stewart DA, Eda G, Mattevi C, et al. Atomic and electronic structure of graphene-oxide. Nano Lett 2009;9:1058–63.
[7] Mohanty N, Berry V. Graphene-based single-bacterium resolution biodevice and DNA transistor: interfacing graphene derivatives with nanoscale and microscale biocomponents. Nano Lett 2008;8:4469–76.
[8] Shan CS, Yang H, Han D, Zhang Q, Ivaska A, Niu L. Water-soluble graphene covalently functionalized by biocompatible poly-L-lysine. Langmuir 2009;25:12030–3.
[9] Liu Z, Robinson JT, Sun X, Dai H. PEGylated nano-graphene oxide for delivery of water insoluble cancer drugs. J Am Chem Soc 2008;130:10876–7.
[10] Lu CH, Zhu CL, Li J, Liu JJ, Chen X, et al. Using graphene to protect DNA from cleavage during cellular delivery. Chem Commun 2010;46:3116–8.
[11] Shijiang H, Song B, Li D, Zhu C, Qi W, Wen Y, et al. Graphene nanoprobe for rapid, sensitive, and multicolor fluorescent DNA analysis. Adv Funct Mater 2010;20:453–9.
[12] Wilson NR, Pandey PA, Beanland R, Young RJ, Kinloch IA, Gong L, et al. Graphene oxide: structural analysis and application as a highly transparent support for electron microscopy. ACS Nano 2009;3:2547–56.
[13] Gómez-Navarro C, Weitz RT, Bittner AM, Scolari M, Mews A, Burghard M, et al. Electronic transport properties of individual chemically reduced graphene oxide sheets. Nano Lett 2007;7:3499–503.
[14] Wang S, Kailian PA, Ziqian W, Tang ALL, Thong JTL, Loh KP. High mobility, printable, and solution-processed graphene electronics. Nano Lett 2010;10:92–8.

[15] Sun X, Luo D, Liu J, Evans DG. Monodisperse chemically modified graphene obtained by density gradient ultracentrifugal rate separation. ACS Nano 2010;4:3381–9.
[16] Sato K, Obinata K, Sugawara T, Urabe I, Yomo T. Quantification of structural properties of cell-sized individual liposomes by flow cytometry. J Biosci Bioeng 2006;102:171–8.
[17] Hirata M, Gotou T, Horiuchi S, Fujiwara M, Ohba M. Thin-film particles of graphite oxide 1: high-yield synthesis and flexibility of the particles. Carbon 2004;42:2929–37.
[18] Gupta R, Chakrabarti P, Dikshit M, Dash D. Late signaling in the activated platelets upregulates tyrosine phosphatase SHP1 and impairs platelet adhesive function: regulation by calcium and src kinase. Biochim Biophys Acta 2007;1773:131–40.
[19] Van Bockstaele F, Janssens A, Piette A, Callewaert F, Valerie P, Offner F, et al. Kolmogorov–Smirnov statistical test for analysis of ZAP-70 expression in B-CLL, compared with quantitative PCR and IgVH mutation status. Cytom B Clin Cytom 2006;70B:302–8.
[20] Gupta A, Chen G, Joshi P, Tadigadapa S, Eklund PC. Raman scattering from high-frequency phonons in supported *n*-graphene layer films. Nano Lett 2006;6:2667–73.
[21] Attal S, Thiruvengadathan R, Regev O. Determination of the concentration of single-walled carbon nanotubes in aqueous dispersions using UV–visible absorption spectroscopy. Anal Chem 2006;78:8098–104.
[22] Luo Z, Lu Y, Somers LA, Johnson AT. High yield preparation of macroscopic graphene oxide membranes. J Am Chem Soc 2009;131:898–9.
[23] Vorauer-Uhl K, Wagner A, Borth N, Katinger H. Determination of liposome size distribution by flow cytometry. Cytometry 2000;39:166–71.
[24] Nakamura M, Ishimura K. Rapid size evaluation of nanoparticles using flow cytometry. Adv Sci Lett 2010;3:130–7.
[25] Sun X, Liu Z, Welsher K, Robinson JT, Goodwin A, Zaric S, et al. Nano-graphene oxide for cellular imaging and drug delivery. Nano Res 2008;1:203–12.
[26] Jung JH, Cheon DS, Liu F, Lee KB, Seo TS. A graphene oxide based immuno-biosensor for pathogen detection. Angew Chem 2010;122:1–5.
[27] Liu F, Choi JY, Seo TS. Graphene oxide arrays for detecting specific DNA hybridization by fluorescence resonance energy transfer. Biosens Bioelectron 2010;25:2361–5.
[28] Goki E, Lin Y, Mattevi C, Yamaguchi H, Chen H, Chen I, et al. Blue photoluminescence from chemically derived graphene oxide. Adv Mater 2009;22:505–9.